

The typical frequency of the $m = 2$ mode was 18 kHz. These MHD properties are similar to those of circular tokamaks.^{5,6}

If we assume that the major axis of the cross section b is reduced effectively to b' due to current shrinking while a is unchanged and that the $m = 2$ mode is a kink mode,⁷ the value of b' can be estimated from Fig. 5 and Eq. (1); the estimated value of b' is 23 cm for $t = 0.8$ msec, giving the elongation degree of 2.3. This is the lower limit since $m = 2$ mode may be (partly or entirely) the resistive tearing mode.⁸

In the latter half of the discharge, there appeared negative voltage spikes (~ -20 V) on the loop voltage (Fig. 4). The magnetic probe signals show the following: (i) These negative spikes occurred when the $m = 2$ oscillations were almost damped down; (ii) these corresponded to the superposition of $m = 0$ expansion in the minor radius and an inward shift in the major radius (~ 2 cm); and (iii) n is 0. An increase of the H_β signal coincided with the negative voltage spike. These observations show that this negative voltage spike is quite similar to the "disruptive instability"^{5,9} familiar in circular tokamaks.

Because of lack of direct measurements of temperature and density, definite statements cannot be made about the β value. However, it is demonstrated experimentally that a D -shaped, elongated configuration at low safety factor q has been obtained by means of active field shaping and that the MHD properties of the discharge are analogous to those of a circular cross-section

tokamak.

*Present address: Plasma Physics Laboratory, Princeton University, Princeton, N. J. 08540.

¹T. Ohkawa, *Kaku Yugo Kenkyu* **20**, 557 (1968); D. Dobbrott and M. S. Chu, *Phys. Fluids* **16**, 1371 (1973); L. A. Artsimovich and V. D. Shafranov, *Pis'ma Zh. Eksp. Teor. Fiz.* **15**, 72 (1972) [*JETP Lett.* **15**, 51 (1972)].

²T. Ohkawa and H. G. Voorhies, *Phys. Rev. Lett.* **22**, 1275 (1969); T. H. Jensen *et al.*, in *Plasma Physics and Controlled Nuclear Fusion Research* (International Atomic Energy Agency, Vienna, 1974), Vol. 1, p. 281.

³A. V. Bortnikov *et al.*, in *Proceedings of the Sixth European Conference on Controlled Fusion and Plasma Physics, Moscow, U. S. S. R., 1973* (U. S. S. R. Academy of Sciences, Moscow, 1973), Vol. 1, p. 165, and in *Proceedings of the Third International Symposium on Toroidal Plasma Confinement, Garching, Germany, March 1973* (Max-Planck-Institut für Plasmaphysik, Garching, Germany, 1973), and in *Plasma Physics and Controlled Nuclear Fusion Research* (International Atomic Energy Agency, Vienna, 1974), Vol. 1, p. 147.

⁴U. Ascoli-Bartoli *et al.*, in *Plasma Physics and Controlled Nuclear Fusion Research* (International Atomic Energy Agency, Vienna, 1974), Vol. 1, p. 191.

⁵J. C. Hosea *et al.*, in *Plasma Physics and Controlled Nuclear Fusion Research* (International Atomic Energy Agency, Vienna, 1971), Vol. 2, p. 425.

⁶S. V. Mirnov and I. B. Semenov, *At. Energ.* **30**, 20 (1971) [*Sov. At. Energy* **30**, 22 (1971)]; K. Makishima *et al.*, *Phys. Rev. Lett.* **36**, 142 (1976).

⁷V. D. Shafranov, *Sov. Phys. Tech. Phys.* **15**, 175 (1970); S. Inoue *et al.*, *Phys. Lett.* **53A**, 342 (1975).

⁸H. P. Furth *et al.*, *Phys. Fluids* **16**, 1054 (1973).

⁹L. A. Artsimovich, *Nucl. Fusion* **12**, 215 (1972).

Pulsed Ion Diode Experiment*

D. S. Prono, J. W. Shearer, and R. J. Briggs

Lawrence Livermore Laboratory, University of California, Livermore, California 94550

(Received 2 March 1976; revised manuscript received 24 May 1976)

Ion current densities up to several kiloamperes per square centimeter and total ion currents ranging from 50 to 150 kA have been produced at voltages of 100–300 kV in a modified relativistic-electron-beam diode. The experiments are in general accord with the predictions of a recent reflex-triode theory.

There has been considerable interest recently in the production of intense ion beams with pulsed diode techniques.¹⁻³ Intense ion flows in the diode regions of electron beam generators have, in fact, been invoked to explain aspects of the observed diode behavior for both self-pinched flows³ and reflex diode configurations.^{2,4-7}

In this Letter, we present results of an experimental study of the ion flow created in the reflex configuration described in Ref. 2. Briefly, this configuration consists of a planar diode immersed in an externally applied axial magnetic field, with a thin anode foil and a virtual cathode beyond the foil that reflects essentially all of the electrons

back into the diode region. Two new experimental results are presented here: First, measurements of the reflex-diode voltage and current as a function of foil thickness show a dependence in general accord with theory² and demonstrate that total currents up to 30 times the Langmuir bipolar flow value are achieved. Second, again in accord with theory, measurements by several techniques verify the presence of intense ion current densities up to several kiloamperes per square centimeter and total ion currents ranging from 50 to 150 kA.

The experiments were carried out on the OWL II generator,⁸ and we used basically the same magnetic field coils, voltage diagnostics, and current loops as the earlier reported work.² To measure ion flow, we added Faraday collectors with self-contained calorimeters, and neutron counting diagnostics. Four Faraday collectors were located within the cathode stalk. Three of these units were radially separated 1 cm behind the cathode and the fourth was axially displaced an additional 25 cm to provide time-of-flight information. All Faraday-collector-calorimeter units viewed the anode foil through $\frac{1}{16}$ -in. holes in the cathode plate. Signal cables from these diagnostics were ducted out through the wall of the second transformer stage of the OWL II generator inside an aluminum pipe which was sufficiently long to provide transit-time isolation⁹ against the negative cathode potential.

The anode foils were made of titanium (0.5–1.0 mil) or Mylar (0.1–2.0 mil, aluminized on the virtual cathode side). They were mounted 9.5 mm from the 3-in.-diam cathode. The anodes were coated on the cathode side with pump oil to serve as a source of H^+ ions, or with 0.2 mg/cm² of CD_2 when D^+ ions were desired. When using the CD_2 -covered anode foil, a deuterium-loaded titanium plate (also with $\frac{1}{16}$ -in. holes) was used as the cathode. Two silver activation counters located just outside the magnetic field coils⁹ were used to detect neutrons from the reaction ${}^2H({}^2H, n){}^3He$ occurring in the cathode. Unless stated otherwise, the virtual-cathode drift space contained ~ 20 mTorr of hydrogen and the longitudinal magnetic field was 16 kG. This slight hydrogen fill in the drift tube was empirically found to aid in the suppression of apparent diode voltage oscillations which reduced ion flow.

Figure 1 shows oscilloscope traces for a proton experiment with a $\frac{1}{2}$ -mil titanium anode; the diode gap voltage signal was corrected for the inductive error² (tube voltage minus LI). The di-

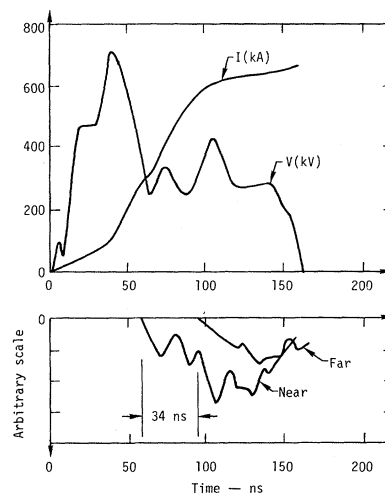


FIG. 1. The oscilloscope wave forms shown are total diode current $I (=I_i + I_e)$, diode gap voltage V , current of near Faraday collector, and current of far Faraday collector. A 0.5-mil titanium anode foil was used with ~ 20 mTorr of hydrogen filling the drift tube.

ode's characteristics show two distinct operational modes. For the first 50 nsec the diode voltage and current behave as a normal $2.5\text{-}\Omega$ diode. However, there follows a transition period during which the total generator current climbs steeply and the diode voltage drops. During this transition the near Faraday collector indicates that ion flow begins. For the remainder of the pulse (from 60 nsec to diode closure at 160 nsec) the diode remains in a new low-impedance mode ($\sim 0.4\ \Omega$) of 650 kA and 280 kV. The delay in the time of arrival at the far Faraday collector corresponds to 280-keV protons, confirming the voltage trace.

Our explanation and that of others⁴ for these two diode operational modes is that sufficient electron beam energy (~ 200 J) must be deposited in the anode foil before it becomes an ion plasma source. Once this anode plasma is well established the theoretically predicted low-impedance ion mode can begin. More than three dozen experiments over the whole range of foil thickness verified this diode impedance transformation coupled with onset of ion emission. Only two exceptions to this result were found. First, when higher hydrogen fill pressures were used in the drift tube the virtual cathode became neutralized well before diode closure; thus electrons ceased being reflected back into the diode and the diode returned to its normal impedance state.² Second, when a solid plate was located in the drift tube approximately one anode tube diameter from the

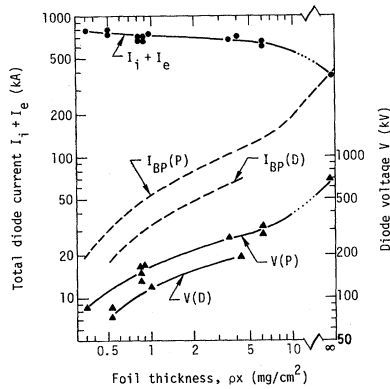


FIG. 2. Measurements of total diode current (●) and voltage (▲) are shown versus anode foil thickness for proton (P) and deuteron (D) experiments. Also shown is the calculated bipolar current. Data points for $\rho x = \infty$ are observed normal diode characteristics with no reflecting electrons. Except for anode foil changes, all experimental conditions are constant.

anode foil the diode also operated only in a normal impedance state. This plate apparently distorted the potential lines forming the virtual cathode and prevented electron reflection.

In Fig. 2 the average reduced voltage and the peak total diode current are displayed as a function of foil thickness; for the thinnest foils the diode impedance dropped to $\sim 0.1 \Omega$. For the purpose of later discussion Fig. 2 also shows the value of the total Langmuir bipolar current I_{BP} for this diode¹⁰:

$$I_{BP} = (1.86A/9\pi)(2e/m)^{1/2} \times [1 + (Zm/M^{1/2})V^{3/2}/d^2], \quad (1)$$

where A is the diode area (45 cm^2), V is measured reduced diode voltage, and d is the anode-cathode gap (taken as $\sim 5 \text{ mm}$, because of diode closure).

In Fig. 3 we show the measurements of average current density as a function of anode foil thickness. These data only represent those shots where anode-cathode spacing was 9.5 mm (to keep pulse duration constant), pulse charge was 2.9 to 3.1 MV (nearly constant tube voltage), and slight H_2 gas fill (20 mTorr) was present in the drift chamber to stabilize the virtual cathode.

Our most reliable measurement of ion current intensity was the neutron diagnostic. The neutron output at 90° from the reaction ${}^2\text{H}({}^2\text{H}, n)\text{He}^3$ was chosen because its cross section is well known, there is no threshold (important for low-energy ions), and the technique is unhampered by the

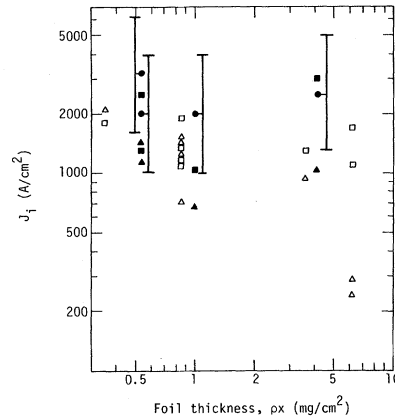


FIG. 3. Displayed are measurements of ion current density versus anode foil thickness for otherwise constant experimental conditions. Various data points are for different diagnostic measurements on the same experiment; clusters of data points are from repeated experiments. ●, ■, and ▲ are, respectively, neutron diagnostics, calorimeter, and Faraday-collector readings for deuteron experiments; □ and Δ are, respectively, calorimeter and Faraday-collector readings for proton experiments.

negative polarity of the cathode. Details of this diagnostic technique are given elsewhere.⁹ To unfold the neutron count in terms of a total current and current density we used the average diode voltage value that was measured during the ion emission phase (Fig. 2) and an ion pulse duration of 50 nsec , and we assumed uniform emission across the 45-cm^2 cathode area. The principal source of error in the neutron diagnostic is the uncertainty of the deuterium-titanium atom ratio within $2 \mu\text{m}$ of the cathode surface, which encompasses the range of the bombarding deuterons.⁹ We estimate that our experimental calibration of this concentration has an uncertainty of ${}^{+100}_{-50}\%$. The shot-to-shot variations of measured neutron output were less than this uncertainty.

Data points for current densities as measured by Faraday cup and calorimeter at 1.5 cm radius are also shown in Fig. 3. Where appropriate, diagnostic output signals were related to J_i using the area of the $\frac{1}{16}$ -in. holes, the measured voltage during ion emission, a 50-nsec pulse duration, and the calibrated sensitivity of the collectors and calorimeters. We cannot state an uncertainty in the calorimeter readings. Although the calorimetric contribution due to radiation can be shown to be negligible, we have no estimate of the anode-cathode plasma energy or how well it coup-

les to the calorimeters through the $\frac{1}{16}$ -in. holes. Uncertainty in Faraday cup readings is also unspecified. Care was taken to zero bias the Faraday collectors relative to the cathode; thus secondary electrons emitted from the collector surface are largely canceled by the slow electrons which must accompany the intense ion flow. However, again because we have no experimental calibration of this effect, we do not ascribe error bars.

A pinhole-camera x-ray picture of a 0.5-mil-titanium-foil experiment showed an axial maximum of intensity. This would be expected since maximum B_θ self-fields are approximately 2.5 times stronger than the applied 16 kG; hence partial beam pinching should result. Anode-foil damage covered a region slightly less than the full cathode area, thus confirming partial beam pinching. Also, signals from the outer Faraday collector at $r = 3$ cm peaked earlier in time (during the steeply rising current phase) and at a lower level than the other collectors. This indicates that ion currents were emitted from the region of the reflexing electrons which in our experiment had helical axial trajectories rather than the one-dimensional trajectories analyzed in theory.² The dominance in our experiment of the reflex ion diode mechanism over that due to beam pinching³ is indicated by the observed voltage dependence upon anode foil thickness, a phenomenon predicted by reflex theory and not expected in pinched-beam ion diodes.

Comparison of these experimental results with the steady-state theory of Ref. 2 is complicated by the fact that the exact shape of the total electron spectrum in the diode region is unknown. This shape depends on scattering and absorption in the foil, and it is also modified at large radii by the fact that $B_\theta > B_z$. For these reasons, the theory uses "model" spectra as the best available approximation to the real situation. But for all model spectra, the theoretical results display two important features: First, large ratios of $(I_e + I_i)/I_{BP}$ occur when the average number of anode transits η of the reflexing electrons is close to the critical maximum η_c ; second, when $\eta \rightarrow \eta_c$, the ion-electron current ratio I_i/I_e should be substantially higher than its bipolar value $(Zm/M)^{1/2}$.

The experimental measurements of diode voltage and current meet the first of the above conditions; Fig. 2 shows that the ratio $(I_e + I_i)/I_{BP}$ is always much greater than unity, ranging from 4 to 30. This result implies that $\eta \approx \eta_c$, which is

the condition for substantial ion currents. The deuterium current measurements (neutron diagnostics for which we have the most confidence) plotted in Fig. 3 confirm that prediction. Using 100 kA as an average value of deuterium ion current I_i , and 700 kA for $I_i + I_e$, then we find $I_i/I_e \approx 0.17$, which is a factor of 10 higher than the bipolar value of this ratio.

A further connection between the experiment and the theory is found from the following expression for the average number of anode transits η :

$$\eta \approx R(v)/3\rho x \approx 0.005V^{3/2}/\rho x, \quad (2)$$

where $R(v)$ is the residual range (milligrams per square centimeter) of an electron of energy eV (kilovolts), ρx is the thickness of the anode foil (milligrams per square centimeter), and the factor 3 is based on Monte Carlo calculations¹¹ which show that half of the electrons penetrate less than one-third of the range. Equation (2) uses an approximate fit to $R(v)$, which is nearly independent of foil material.¹²

Since $\eta \approx \eta_c$, and since Monte Carlo calculations¹¹ suggest that the electron energy spectrum should not change rapidly with foil thickness, we should expect that η_c is approximately a constant for different foil thicknesses. Thus, from Eq. (2) one finds the scaling relation $V \sim (\rho x)^{2/3}$. A slow increase of reduced diode voltage with foil thickness is observed (Fig. 2) which is close to this prediction.

From Eq. (2) and Fig. 2, we find $2 \leq \eta \leq 5$. This result and the ratio $I_i/I_e = 0.17$ are both consistent with an axial electron energy spectrum which is intermediate between the model spectra *A* and *B* of Ref. 2. This suggests that the spectrum is weighted towards low energies, as might be expected for significant electron scattering. Further work is needed to evaluate the effects of different foil materials and thickness on spectrum shape and η_c , which determine diode voltage and efficiency parameters.

These results demonstrate a new low-impedance mode of operation of high-current diodes which is connected with the generation of intense ion currents and confirms the essence of a steady-state theory of reflex-diode operation.² Important parameters, such as the divergence angle of the ion beams, have not yet been determined. Nevertheless, it seems quite probable that continued development of this technology could produce intense pulsed ion beams that would have important applications such as the initiation of field reversal or energetic plasma startup for

mirror-confined plasmas.

We thank Edward Chambers, Dave Trimble, Howard Storms (General Electric Co.), and Charles Wright (Physics International) for their assistance with the experiment.

*Work performed under the auspices of the U. S. Energy Research and Development Administration under contract No. W-7405-Eng-48.

¹S. Humphries, J. J. Lee, and R. N. Sudan, *J. Appl. Phys.* **46**, 187 (1975).

²J. M. Creedon, I. D. Smith, and D. S. Prono, *Phys. Rev. Lett.* **35**, 91 (1975); D. S. Prono, J. M. Creedon, I. Smith and N. Bergstrom, *J. Appl. Phys.* **46**, 3310 (1975); T. M. Antonsen, Jr., and E. Ott, *J. Appl. Phys. Lett.* **28**, 424 (1976).

³J. W. Poukey, *J. Vac. Sci. Technol.* **12**, 1214 (1975); S. A. Goldstein and R. Lee, *Phys. Rev. Lett.* **35**, 1079

(1975).

⁴M. DiCapua, R. Huff, and J. Creedon, in Sandia Laboratory Report No. SAND 76-5122, Vol. I, p. 555 (to be published).

⁵D. S. Prono, J. W. Shearer, and R. J. Briggs, in Sandia Laboratory Report No. SAND 76-5122, Vol. I, p. 575 (to be published).

⁶P. A. Miller, C. W. Mendel, D. W. Swain, and S. A. Goldstein, in Sandia Laboratory Report No. SAND 76-5122 Vol. I, p. 619 (to be published).

⁷J. Golden, C. A. Kapetanacos, R. Lee, and S. A. Goldstein, in Sandia Laboratory Report No. SAND 76-5122, Vol. I, p. 635 (to be published).

⁸G. B. Frazier, *J. Vac. Sci. Technol.* **12**, 1183 (1975).

⁹J. W. Shearer and D. S. Prono, Lawrence Livermore Laboratory Report No. UCID-17070, 1976 (unpublished).

¹⁰I. Langmuir, *Phys. Rev.* **33**, 954 (1929).

¹¹S. M. Seltzer and M. J. Berger, *Nucl. Instrum. Methods* **119**, 157 (1974).

¹²R. D. Evans, *The Atomic Nucleus* (McGraw-Hill, New York, 1955), p. 611 ff.

Hydrogen Tunneling States in Niobium*

H. K. Birnbaum

*Department of Metallurgy and Mining Engineering and Materials Research Laboratory,
University of Illinois at Urbana-Champaign, Urbana, Illinois 61801*

and

C. P. Flynn

*Department of Physics and Materials Research Laboratory, University of Illinois at Urbana-Champaign,
Urbana, Illinois 61801*

(Received 29 March 1976)

The known low-temperature properties of H and D in Nb are explained by a model of tunnel-split pocket states.

The structure and diffusive properties of H centers in metals have recently become the focus of renewed interest due in part to the nonclassical nature of several observed properties. Even for the best-studied case of dilute solutions of H in Nb, however, the local structure of the H impurity has remained a puzzle. In this Letter we show that the known properties of H and D in Nb possess a consistent and satisfactory interpretation in terms of a system of tunnel-split pocket states.

Our discussion employs octahedral (o), tetrahedral (t), and triangular (τ) interstitial sites of the bcc lattice, distinguished by differing symbols in Fig. 1(a). H diffuses by hopping even at low temperatures¹; it therefore seems probable that self-trapping localizes these impurities. For this reason we suppose that a H wave func-

tion centered on one site may spread onto *dissimilar* neighboring sites only. Figures 1(b)–1(d) show the octahedral-, tetrahedral-, and triangular-centered orbital systems that follow from these assumptions. In the remainder of this Letter we examine the consequences of these ideas for the specific case of H and D in Nb.

The observations to be explained are as follows: (a) Large deviations from a harmonic Debye-Waller broadening appear in neutron quasi-elastic-scattering results,^{2,3} which can be analyzed as the sum of *two* rms amplitudes, ~ 0.14 and ~ 1 Å, respectively. (b) Heat-capacity⁴ and thermal-resistance⁵ anomalies occurring in Nb-H and Nb-D dilute solutions at $\sim 1^\circ\text{K}$ exhibit marked nonclassical isotope effects. (c) Neutron structure analysis⁶ and diffuse scattering⁷ have